Sains Malaysiana 53(9)(2024): 3097-3111
http://doi.org/10.17576/jsm-2024-5309-15

Analysis of Schlemm's Canal Measurement and Evaluation with Fourier-Domain Optical Coherence Tomography in Primary Open-Angle Glaucoma

(Analisis Pengukuran dan Penilaian Saluran Schlemm dengan Tomografi Koheren Optik Fourier-Domain dalam Glaukoma Sudut Terbuka Primer)

SUCIJANTI[1], ZHI LAN YUAN[1,*], YA LIANG[1], SUN HONG[1], LIU WEI GU[1] & SI ZHENLI[2]

[1]*Department of Ophthalmology, First Affiliated Hospital of Nanjing Medical University, Nanjing, Jiangsu Province, China*

[2]*Department of Ophthalmology, Nanjing Tongren Hospital, Nanjing, Jiangsu Province, China*

Received: 18 November 2023/Accepted: 17 July 2024

ABSTRACT

The most common cause of permanent vision loss or blindness in the world is glaucoma. Primary Open Angle Glaucoma (POAG) develops when the eye drainage canals clog over time, increasing intraocular pressure and damaging the optic nerve. In POAG, an ophthalmology examination usually shows an open anterior chamber and chronic, irreversible multifactorial optic neuropathy followed by central visual field loss. OCT is specifically employed to investigate the elasticity of tissue, particularly in Schlemm's canal. This study aims to analyzed the morphological parameters of Schlemm's canal among patients with POAG and normal healthy control. In this observational study, we included one hundred patients, among them 50 patients had POAG, and 50 healthy controls, and both eyes were assessed. We measured the study cohort's and the healthy cohort's eyes' elevated IOP and the Schlemm's canal cross-sectional area (CSA). RT-Vue OCT was used to analyze both eyes' temporal, superior, inferior, and nasal regions. The data were analyzed using both univariate and bivariate methods. The characteristics of the morphological measurement of Schlemm's canal results were similar to those of Kagemann et al. There was a significant difference between age and SC measurement, but no correlation was observed between SC measurement and IOP or visual acuity. OCT is a useful way to evaluate the morphological status of Schlemm Canal in glaucoma patients. The eyes with POAG had smaller Schlemm's Canal- CSA than the normal eyes. The Schlemm canal-CSA in Chinese people had no differences from that of peoples of other races.

Keywords: Glaucoma; intraocular pressure; OCT; Schlemm's canal; visual acuity

ABSTRAK

Penyebab paling biasa kehilangan penglihatan kekal atau buta di dunia adalah glaukoma. Glaukoma Sudut Terbuka Primer (POAG) berkembang apabila saluran saliran mata tersumbat dari masa ke masa, meningkatkan tekanan intraokular dan merosakkan saraf optik. Dalam POAG, pemeriksaan oftalmologi biasanya mendedahkan ruang anterior terbuka dan neuropati optik multifaktorial kronik yang tidak dapat dipulihkan diikuti dengan kehilangan medan penglihatan pusat. OCT digunakan secara khusus untuk mengkaji keanjalan tisu, terutamanya dalam saluran Schlemm. Kajian ini bertujuan untuk menganalisis parameter morfologi saluran Schlemm dalam kalangan pesakit POAG dan kawalan sihat normal. Dalam kajian pemerhatian ini, kami memasukkan seratus pesakit, antaranya 50 pesakit mempunyai POAG dan 50 kawalan sihat dengan kedua-dua mata telah dinilai. Kami mengukur IOP kohort kajian dan mata kohort yang sihat dan kawasan keratan rentas kanal Schlemm (CSA). RT-Vue OCT digunakan untuk menganalisis kawasan temporal kedua-dua mata, superior, inferior dan hidung. Data dianalisis menggunakan kaedah univariat dan bivariat. Ciri pengukuran morfologi hasil kanal Schlemm adalah serupa dengan ciri Kagemann et al. Terdapat perbezaan yang signifikan antara umur dan pengukuran SC, tetapi tiada korelasi diperhatikan antara pengukuran SC dan IOP atau ketajaman penglihatan. OCT adalah cara yang sesuai untuk menilai status morfologi kanal Schlemm pada pesakit glaukoma. Mata dengan POAG mempunyai Kanal Schlemm - CSA yang lebih kecil daripada mata biasa. Kanal Schlemm-CSA dalam kalangan kaum Cina tidak mempunyai perbezaan daripada kaum lain.

Kata kunci: Glaukoma; Saluran Schlemm; ketajaman visual; OCT; tekanan intraokular

INTRODUCTION

Across the globe, glaucoma causes irreversible visual impairment or blindness (Bourne et al. 2013). About 60% of all instances of glaucoma worldwide are in Asia (Foster & Johnson 2001; Quigley & Broman 2006; Tham et al. 2014; Wong, Loon & Saw 2006). In addition, compared to East Asia, South-Central Asia is predicted to have the most significant number of cases of Primary Open Angle Glaucoma (POAG), secondary glaucoma, and overall Glaucoma by 2040 (UNP 2013). Among the glaucoma subtypes, POAG is the most prevalent. A sign of POAG is the loss of retinal ganglion cells and their axons. POAG is an open anterior chamber with increased intraocular pressure (IOP), the most common cause of irreversible blindness worldwide (Caprioli 2007; Caprioli & Coleman 2008; Resnikoff et al. 2004).

The major risk factor for POAG is elevated intraocular pressure (IOP), consistently controlled by balancing aqueous humor production by the ciliary body with drainage through the structures located at the junction where the cornea meets the iris (Tamm, Braunger & Fuchshofer 2015) and 75% to 80% of aqueous humor flows through the traditional pathway, which is composed mainly of the trabecular meshwork (TM) and Schlemm's canal (SC) (Kuehn et al. 2021).

The location at the corneal scleral limbus, an elliptical shape with an inner wall connecting the Juxta Canalicular Tissue (JCT) and the outer wall directly to the sclera, is called Schlemm's canal, also known as the scleral venous sinus. A ring tubule there serves as the channel for the passage of aqueous humor (Luo 2010). The channel SC at the anterior chamber angle where AH enters the bloodstream was discovered in 1830 by the German anatomist Friedrich Schlemm (Dvorak-Teobald 1955; Mansouri & Shaarawy 2015). The juxtacanalicular trabecular meshwork is located on the right next to the ring-shaped canal, which surrounds the cornea and has a length of 36-40 mm (Byszewska et al. 2019; Daurtriche et al. 2015; Parc & Johnson 2003). Draining AH from the trabeculum to the CC is one of the leading roles of the SC. Not every SC cell is the same despite being situated next to the trabeculum (Lai et al. 2019; Vahabikashi et al. 2019). In cross-section, SC has the shape of an elongated ellipse, its longer axis measuring 150-350 μm. 3D visualizations have enabled canal measurements, and the cross-sectional area ranges from 4064 to 7164 μm^2 (Kagemann et al. 2014a, 2014b, 2011). The inner and outer walls of the canal may be distinguished from one another due to their unique microanatomy, as each is composed of a single, continuous layer of endothelium. Both walls' cells have diverse morphologies, organelles, expression of several markers, and functions (Hamanaka et al. 2016; Karl et al. 2005). Since the inner wall provides the most significant resistance to AH drainage, it is explored regularly (Fan et al. 2020; Osmond, Krebs & Pantcheva 2020; Vranka et al. 2015).

Imaging technology known as optical coherence tomography (OCT) has advanced development over the last ten years. It operates on the fundamental ideas of a coherent lower-light interferometer. By using multiple scattering signals or back reflection, one can see biological tissue in two or three dimensions by detecting weak coherent light incident on different depth layers of the tissue (Chen et al. 2014).

TM motion is being clarified in novel ways using optical coherence tomography (OCT) imaging, which shows that TM motion deviates in glaucoma. Human imaging shows that IOP controls the TM's enlargement into the SC (Kagemann et al. 2015). Recent data indicates that aberrant responses in glaucoma are by OCT (Gao et al. 2020). Additional high-resolution OCT (HR-OCT) investigations show that the lumen dimensions of the collector channel (CC) and SC vary in tandem with changes in pressure in real time (Hariri et al. 2014; Xin et al. 2017, 2016). Similar structures in the TM routes are found by these OCT studies, scanning electron microscopy, and micro-CT (Bentley, Hann & Fautsch 2016; Hann et al. 2011; Johnstone 2018). There is no study to date has reported on the circumferential morphological measurement of Schlemm Canal in POAG and healthy normal eyes. And there is still no clinical observation evidence supporting the hypothesis that SC constriction, larger or smaller, can lead to the elevation of IOP in patients with POAG. We investigated the tissue elasticity by measuring SC width, diameter, and length in four quadrants: nasal, inferior, temporal, and superior. Thus, this study aimed to compare SC's normal and POAG circumferential morphological status with RT-Vue OCT.

MATERIALS AND METHODS

STUDY SUBJECTS

This study is an analytical observational study with a prospective design. We employed a convenient sampling strategy in the sample selection process. The subjects were Nanjing residents who participated in Prof. Yuan Zhilan's glaucoma clinic at Jiangsu Province Hospital, China. Before participating in the study, subjects signed an informed consent form. The study took place from May 2020 to September 2022. The First Affiliated Hospital of Nanjing Medical University's Ethics Committee accepted the study protocol (No.2019-SR-457). In addition, we adhered to the principles of the Declaration of Helsinki. This trial was registered in the Chinese Clinical Trial Registry (ChiCTR1900028618, December 29, 2019).

We included individuals who met the following criteria in the study: they had been diagnosed with primary open-angle glaucoma (POAG); they had at least two intraocular pressure measurements that were greater than 21 mmHg; they had glaucomatous optic neuropathy; were between the ages of 20 and 80; The anterior chamber angle is open and had elevated intraocular pressure under the condition of maximum medication that could still cause further damage

to the optic nerve. Exclusion criteria for the research were: the presence of neovascular glaucoma (secondary glaucoma, hormonal glaucoma, pigmented glaucoma); Uveitis; The anterior chamber angle is closed and the anterior chamber angle structure is transparent; severe heart and lung diseases and advanced cancer; having a history of mental illness; previous history of trauma or other internal eye surgery; combined glaucoma with ocular or other congenital abnormalities.

SCHLEMM'S CANAL MEASUREMENT

Schlemm's Canal (SC) is an annular chamber aqueous discharge channel within the scleral groove. SC performs the duties of a compressible chamber. Its appearance and actions indicate that it is part of a lymphatic-like pump that controls intraocular pressure (Johnstone et al. 2021). According to numerous studies and lines of evidence, there is pulsatile flow to the aqueous veins, and the distal outflow channels and SC are the source of the aqueous that induces pulsatile flow (Khatib et al. 2019; Lusthaus et al. 2021). Spectral-domain optical coherence tomography (RT-Vue OCT) indicates that Schlemm's canal (SC) cross-sectional area (CSA) decreases in proximity to collector channel ostia or SC-collector channel branching sites. In particular, SC CSA drops slightly within 160 μm of an ostium, but along the circumferential arc, SC CSA drops by 50%. Numerous articles have measured SC morphology after that time, but none have addressed the fast fluctuations in SC CSA (Chen et al. 2013; Day et al. 2013; Hong et al. 2013; Shi et al. 2012; Wang et al. 2012).

The individuals were directed to face an externally fixed light source during the Schlemm's canal Anterior Segment OCT imaging to center their iridocorneal angle inside the instrument's field of view. The cross-sectional angle images for the Fourier-Domain OCT scans were obtained at four different places within each eye: the angles scanned in one image at three, nine, six, and twelve o'clock, respectively. These angles of each eye represented the nasal, temporal, superior, and inferior of each eye. Four photos were selected for the final study based on image quality after each spot was scanned more than three times. Two skilled ophthalmologists chose every picture in Figures 1, 2, and 3 to assure dependability.

STATISTICAL ANALYSIS

For the analysis, we used the statistical program SPSS. We investigated the Schlemm canal's length or diameter, width, area, angle, and mean and standard deviations for each azimuth. To determine the gender and age differences among POAG patients, we conducted bivariate analysis on Schlemm canal area, width, diameter, and angle measurements in all directions using the student T-test, Mann Whitney U-Test, and Wilcoxon test. When POAG patients had intraocular pressure and visual acuity, Spearman correlation analysis was used to examine the relationship between Schlemm canal parameters of area, width, diameter, and angle. At $p<0.05$, we carried out all statistical analyses.

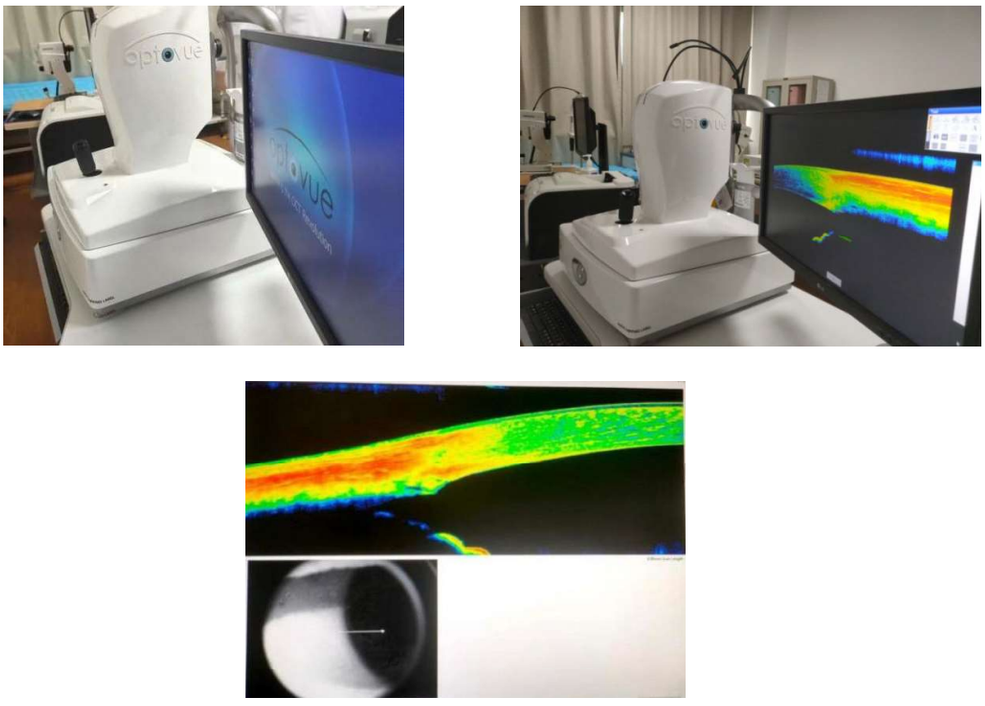

FIGURE 1. Fourier-Domain Anterior Segment OCT is used to image Schlemm's Canal

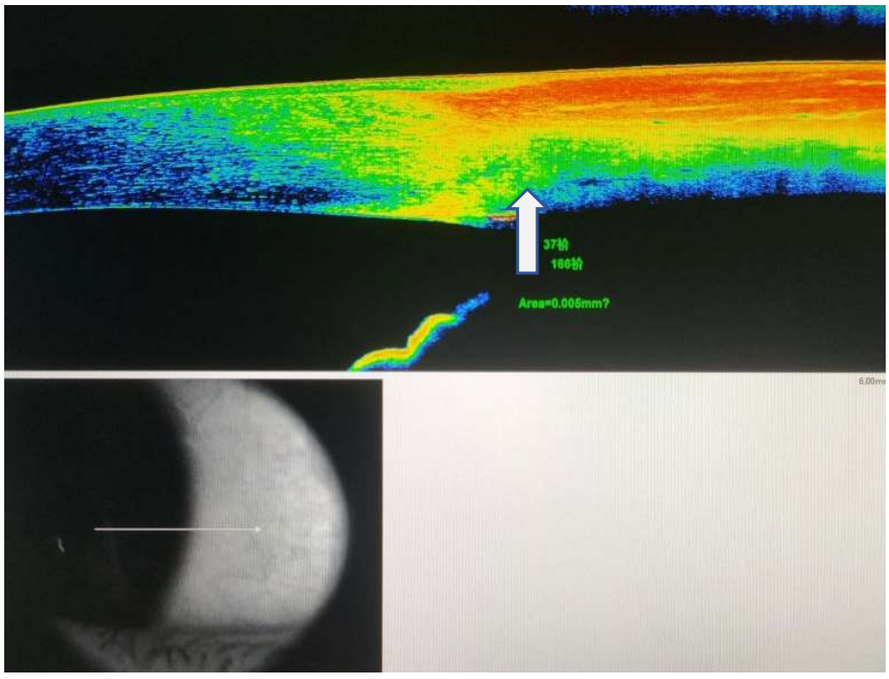

FIGURE 2. The measurement results of the Schlemm's Primary Open Angle Glaucoma canal area. The Cross Sectional Area is 0.005 μm

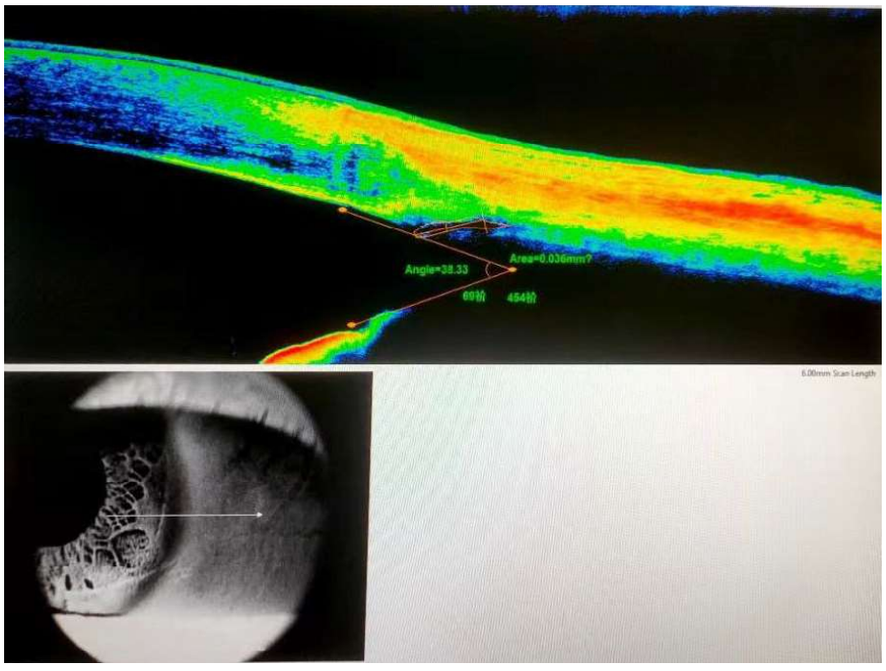

FIGURE 3. Anterior segment OCT image acquisition. The measurement results ofthe Schlemm's canal area in the normal eye. Overlapping volume scans (15- × 2-deg scan angle and 128 B-scans each) were taken in each position (superior, inferior, temporal, nasal, superior-temporal, superior-nasal, inferior-temporal, and inferior-nasal). Scale bar = 1 mm

RESULTS AND DISCUSSION

Anterior Segment RT-Vue Fourier- Domain OCT was used to image the anterior chambers of the right and left Schlemm's canals and to measure visual acuity, intraocular pressure (IOP), and Schlemm's canal area in 200 eyes belonging to 50 participants with POAG and 50 healthy control both eyes. Table 1 displays the demographics of POAG subjects. The average age of the Demographics data POAG participants, 31 males (62%) and 19 females (38%), ranging from 20 to 80 years old, was 52.2 ± 15.1 years. The intraocular pressure in the right eye is 20.3 ± 8.2 mmHg, whereas the left is 18.7 ± 5.5 mmHg. The mean visual acuity (LogMar) for the right and left eyes is 4.2 ± 1.4 and 4.4 ± 2.1, respectively.

There was evidence of Schlemm's canal in diameter and gender. The SC diameter for every patient's Schlemm's canal measurement ranged from 60.93 μm to 297.16 μm in the various eye quadrants, with the highest SC area found on the superior side (Table 2). The characteristics of morphological measurement of Schlemm's canal results are similar to those of Kagemann et al.

There was evidence of Schlemm's canal in every area of the eye. We also examined Schlemm's canal characteristics according to age. There was no significant age difference in the area, width, diameter, or angle. However, following the Spearman correlation test, we discovered a variation in the relationship between Schlemm's canal area, diameter, angle, and age. The SC diameter varied from 61.3 μm to 297.16 μm in the different quadrants of the eye. The SC area was between 63 μm^2 and 194 μm^2. The statistical analysis showed that in all POAG subject comparisons of Schlemm's canal on each side and gender, the left and right eye association with IOP and visual acuity was the same ($P>0.05$).

The demographic data was collected from 100 POAG eyes and 100 control eyes. The average age of the 100 normal control subjects was 26 males (52%) and 24 females (48%), ranging from 20 to 80 years old; the mean age was 46.5 ± 14.4 years. The intraocular pressure in the right eye is 14.4 ± 2.3 mmHg, whereas the left is 14.3± 1.9 mmHg. The mean visual acuity (LogMar) for the right and left eyes is 0.92±0.2 and 0.89±1.1, respectively. Schlemm's canal was measured in all positions 100% in the right eye and left eye.

Significant differences in SC parameters were observed between patients with POAG and normal controls (Table 6). Based on the RT-Vue OCT Schlemm's canal measurement imaging, the average diameter of SC in normal controls is 42.736 ± 11.847 μm, and the average diameter of SC in POAG patients is 22.944 ± 97.548 μm. Both area and diameter area of SC were significantly smaller in POAG participants compared to normal controls (both $p < 0.001$). Lastly, representative SC tables obtained from control and POAG eyes are shown in Table 6.

By enabling the evaluation of Schlemm's canal angle architecture, OCT has advanced imaging resolution and comprehension while helping us better grasp the structural and pathological aspects of Schlemm's canal in vivo. According to SD-OCT, patients with POAG had acceptable visualization and definition of SC. The substitute technology is called ultrasound bio-microscopy (UBM). It studies the Schlemm's canal sizes in the nasal, temporal, superior, and inferior regions (Bentley, Hann & Fautsch 2016; Hann et al. 2011; Johnstone 2018). While UBM can provide reliable and easy-to-use imaging of the Schlemm's canal in all regions, the contact examination procedure might cause eye discomfort or even damage the cornea. During the UBM examination, we applied an external force to the eyeball. This has an impact on the Schlemm's canal size of the scans. Thus, the RT-Vue anterior segment OCT is a safer and more accurate approach for clinical assessment and is used in our study.

Yan et al. (2016a, 2016b) found Schlemm's canal in the superior and inferior quadrants in 2016. The observation rate in normal individuals was 80.3%. Our findings indicated that the nasal quadrant had the maximum Schlemm's canal area, whereas the superior quadrant had the lowest. The significance of SC area and angle decreased with age in POAG subjects in our study. This matched exactly with a research section on the histopathology of Schlemm's Canal on donor eyes (Ainsworth & Lee 1990; Boldea, Roy & Mermoud 2001).

We further hypothesized that several factors could account for the reduced SC area and lower SC detection rates observed in the older patients: (1) SC shrinkage may be the result of SC degeneration itself; (2) decreased traction on SC may be the result of age-related loss in ciliary muscle activity and a changed limbal corneoscleral contour; and (3) there would be less flow into SC as aqueous output declines with age (Ainsworth & Lee 1990; Grierson, Howes & Wang 1984). Finally, there would be less flow into SC as aqueous output declines with age, leading to a continuous reduction in SC area (Becker 1958).

According to research by Hong et al. (2013), the SC and TM properties differed in the various eye quadrants. At the same time, in this POAG study, the SC diameter or area between the nasal and temporal quadrants is similar. This similarity is consistent with the previous description that acknowledged a very variable result. On the other hand, the researchers found temporal SC regions to be substantially smaller than nasal ones.

According to research by Battista et al. (2008) and Gong et al. (2012), when intraocular pressure increases in POAG patients, the inner wall of the Schlemm canal may hernia into the entrance of the collecting tube on the outer wall of the Schlemm's canal in addition to exhibiting collapse symptoms. The part of the inner wall that penetrates the collector tube aperture does not retreat

even when intraocular pressure drops. The pigment level is considerably lower near the collecting canal opening when there is an inner wall hernia.

In vitro healthy eye experiments, Zhu et al. (2013) showed that increased intraocular pressure would lead the Schlemm canal's inner wall to hernia into the broth opening. However, the infested inner wall may escape through the collection opening when the intraocular pressure returns to normal, allowing the Schlemm canal to normalise. Based on this research, the three main elements that lead to the formation of resistance in the Schlemm Canal are its diameter area, its open or active segments, and the entrance of the inner wall hernia into the collection canal. These, however, were absent from our investigation, indicating that the collapse of SC would be a late-stage outcome. We did not check the patient's previous medication regimen because every medicine taken with POAG participants similarly influenced SC measurement and IOP results.

TABLE 1. Demographics data of POAG patients included in this study

	Age					Total
	20-30 year	31-40 year	41-50 year	51-60 year	60+year	
Number of participants	5	5	14	8	18	50
Male/Female	4/1	5/0	10/4	3/5	9/9	31/19
Age	26.8±4.6	34.2±2.7	44.9±2.9	55.3±1.0	68.6±5.2	52.2±15.1
IOP (mmHg)						
Right eyes	21.8±7.3	21.5±9.1	21.3±9.0	20.4±9.6	18.9±7.6	20.3±8.2
Left eyes	20.3±5.9	19.5±2.3	18.7±7.4	17.6±4.4	18.5±5.1	18.7±5.5
Visual Acuity (LogMar)						
Right eyes	4.3±0.6	4.9±0.1	3.8±1.9	4.1±1.7	4.5±1.1	4.2±1.4
Left eyes	4.3±0.6	4.8±0.1	4.1±1.6	4.7±0.2	4.3±1.1	4.4±1.1

Data presented as Mean±SD.*Schlemm's canal was observed in all eye sections.
For all patients with the measurement Schlemm's Canal, the S.C. diameter varied from 60.13 μm, and the S.C. area in the superior was the largest

TABLE 2.Comparison between Schlemm's canal diameter and gender

Diameter (μm)	Gender		Correlation
	Male	Female	p
Right			
N	247.65±102.63	253.47±119.57	0.984
T	215.58±64.04	200.79±83.11	0.246
S	297.16±111.32	271.42±141.08	0.215
I	267.68±118.59	251.58±162.61	0.308
Left			
N	233.16±111.11	203.00±60.93	0.764
T	227.03±124.66	227.74±85.97	0.712
S	274.87±104.37	288.79±72.61	0.358
I	229.48±77.89	234.84±66.19	0.653

The data is expressed in the standard deviation of the mean ±SD; $P < 0.05$ indicates statistical significance.
The statistical analysis showed no significant differences in each diameter and gender of the POAG participants' left and right eyes

TABLE 3. Comparison between POAG Schlemm's canal measurements with age

		Age					Correlation	
		20-30 year	31-40 year	41-50 year	51-60 year	65+year	*r*	*P*
Angle (^{0})								
Right eyes								
	Nasal	32.9±15.7	31.2±4.0	32.5±8.5	22.4±5.6	23.8±10.4	-0.52	0.00*
	Temporal	38.8±16.7	32.3±4.9	33.0±8.4	20.1±6.7	21.6±6.3	-0.62	0.00*
	Superior	34.2±7.5	29.6±3.7	29.6±9.3	20.0±6.8	21.8±10.0	0.48	0.00*
	Inferior	35.8±16.2	29.5±8.6	33.0±11.2	23.5±9.4	25.4±8.7	-0.38	0.01*
Left eyes								
	Nasal	44.0±12.5	27.8±2.4	31.3±10.1	23.1±7.8	25.3±11.6	-0.49	0.00*
	Temporal	39.2±4.9	29.0±5.5	33.2±11.0	22.7±11.0	26.5±9.4	-0.38	0.01*
	Superior	38.1±13.7	25.4±2.7	31.7±11.6	24.7±12.2	26.4±9.8	-0.28	0.05
	Inferior	36.2±8.8	31.4±9.4	30.3±10.8	24.4±9.4	25.3±8.7	-0.40	0.00*
Area (μm^2)								
Right eyes								
	Nasal	70.000±60.000	60.000±10.000	70.000±70.000	60.000±20.000	120.000±20.000	0.09	0.52
	Temporal	40.000±20.000	70.000±40.000	60.000±50.000	60.000±40.000	90.000±140.000	0.01	0.95
	Superior	70.000±50.000	15.000±90.000	80.000±60.000	100.000±70.000	150.000±170.000	0.13	0.36
	Inferior	70.000±50.000	90.000±60.000	100.000±80.000	100.000±110.000	80.000±70.000	0.32	0.02*
Left eyes								
	Nasal	60.000±50.000	40.000±20.000	70.000±50.000	60.000±30.000	50.000±30.000	0.20	0.15
	Temporal	40.000±20.000	130.000±180.000	70.000±60.000	60.000±40.000	60.000±50.000	0.03	0.83
	Superior	70.000±30.000	60.000±40.000	90.000±50.000	130.000±90.000	90.000±50.000	0.26	0.07
	Inferior	50.000±20.000	90.000±60.000	80.000±80.000	80.000±30.000	80.000±40.000	0.28	0.05

continue to next page

continue from previous page

Width (μm)								
Right eyes								
	Nasal	52.0±12.7	42.6±9.0	55.5±35.6	37.9±15.5	68.2±57.4	0.09	0.54
	Temporal	34.4±8.4	52.6±24.7	44.8±13.5	49.4±36.4	57.9±49.3	0.06	0.70
	Superior	44.6±15.0	61.0±23.9	46.0±13.9	65.8±39.0	57.7±26.1	0.16	0.26
	Inferior	62.0±32.6	52.6±16.0	51.6±20.4	46.4±16.9	59.6±37.0	-0.01	0.94
Left eyes								
	Nasal	47.0±8.6	41.0±12.8	56.5±29.6	40.1±12.0	41.9±10.2	-0.18	0.22
	Temporal	36.8±17.2	54.4±32.0	47.6±18.7	54.5±41.3	51.7±30.0	0.08	0.57
	Superior	47.8±13.0	56.0±28.6	45.5±16.2	58.3±18.0	56.8±16.4	0.25	0.08
	Inferior	84.0±63.8	58.8±12.9	55.9±38.9	48.3±10.7	56.9±25.0	0.09	0.55
Diameter (μm)								
Right eyes								
	Nasal	231.2±134.0	216.4±73.0	245.5±106.7	262.4±58.6	262.2±132.2	0.14	0.35
	Temporal	156.8±42.5	236.8±58.2	220.5±68.6	188.5±55.1	218.6±84.9	0.05	0.74
	Superior	217.6±118.9	326.0±107.0	264.2±119.9	293.8±89.1	311.2±142.1	0.15	0.29
	Inferior	221.0±86.8	264.8±137.2	280.4±107.5	236.3±158.3	268.5±162.8	0.01	0.97
Left eyes								
	Nasal	242.4±170.6	207.0±135.5	231.4±98.8	232.0±62.1	207.9±74.9	0.06	0.69
	Temporal	220.2±111.6	293.6±260.4	203.1±80.2	244.4±66.6	222.1±87.6	0.02	0.86
	Superior	227.2±102.0	219.4±58.4	247.4±73.2	355.3±105.6	303.9±83.4	0.41	0.00*
	Inferior	194.6±75.0	271.8±116.3	216.2±71.2	272.1±56.8	224.4±61.3	0.02	0.87

The data have been presented as the Mean±SD

*The statistical analysis and age group are statistical differences on many sides. There is a significant difference between Schlemm's canal width, area, diameter, and angle in the left and right eye correlation with Age ($P < 0.05$) with the Spearman correlation test. The SC diameter varied from 61.3 μm to 297.16 μm in the different quadrants of the eye, and the S.C. area in the superior was the largest. S.C.'s area ranged from 63 μm^2 to 194 μm^2

TABLE 4. Comparison between POAG participants Schlemm's canal measurement with IOP or visual acuity

		mean±SD	Correlation with IOP		Correlation with visual acuity	
			R	p	r	p
S.C. width (μm)						
Right eyes						
	Nasal	55.6±40.8	-0.01	0.95	0.09	0.53
	Temporal	50.0±34.6	0.11	0.44	-0.16	0.28
	Superior	54.7±25.1	-0.13	0.38	0.22	0.12
	Inferior	54.8±27.6	-0.19	0.19	0.08	0.60
Left eyes						
	Nasal	46.1±18.8	0.03	0.82	0.10	0.47
	Temporal	50.0±28.0	0.06	0.68	0.05	0.73
	Superior	52.9±17.9	-0.04	0.79	-0.03	0.85
	Inferior	58.1±32.7	0.08	0.59	-0.00	0.98
SC area (μm^2)						
Right eyes						
	Nasal	90.00±13.00	0.07	0.65	0.01	0.96
	Temporal	70.00±90.00	0.02	0.87	0.02	0.88
	Superior	110.00±12.00	-0.16	0.26	0.20	0.17
	Inferior	90.00±70.00	0.01	0.97	-0.04	0.79
Left eyes						
	Nasal	60.00±40.00	-0.18	0.21	0.09	0.52
	Temporal	70.00±70.00	-0.05	0.73	-0.05	0.72
	Superior	90.00±60.00	-0.10	0.47	0.05	0.74
	Inferior	80.00±50.00	-0.14	0.32	-0.02	0.90
SC diameter (μm)						
Right eyes						
	Nasal	250.0±108.2	-0.02	0.89	-0.04	0.77
	Temporal	210.0±71.4	-0.09	0.56	0.20	0.17
	Superior	287.4±122.7	-0.18	0.21	0.14	.032
	Inferior	261.6±135.6	-0.04	0.78	-0.04	0.81
Left eyes						
	Nasal	221.7±95.6	-0.13	0.36	0.11	0.45
	Temporal	227.3±110.6	0.06	0.67	-0.04	0.77
	Superior	280.2±93.0	0.08	0.57	-0.00	1.00
	Inferior	231.5±73.0	-0.05	0.71	-0.10	0.48

continue to next page

continue from previous page

SC angle						
Right eyes						
	Nasal	27.7±10.2	0.01	0.95	0.14	0.33
	Temporal	27.4±10.5	-0.04	0.76	0.09	0.55
	Superior	25.7±9.7	0.01	0.96	0.13	0.35
	Inferior	28.7±10.9	-0.02	0.92	0.12	0.39
Left eyes						
	Nasal	28.8±11.5	0.08	0.58	-0.06	0.69
	Temporal	29.3±10.4	0.11	0.46	0.12	0.41
	Superior	28.7±11.1	0.04	0.78	0.12	0.42
	Inferior	28.2±9.9	0.09	0.53	0.15	0.29

The data is expressed in the standard deviation of the Mean±SD.
*Statistically, there was no significant difference between Schlemm's canal width, area, diameter, and angle in the Left and Right eye correlation with IOP and visual acuity (P > 0.05) with the Spearman correlation test

TABLE 5. Demographics Data of POAG and Normal participants included in this study

Parameter	POAG	Normal control	*P*
Number of Participants (eyes)	50 (100)	50 (100)	-
Mean Age (S.D.) years	52.2±15.1	46.5 ± 14.4	< 0.005*
Gender, male/ female	31/19	26/24	
IOP (S.D.), mmHg			
Right eyes	20.3±8.2	14.4 ± 2.3	< 0.005*
Left eyes	18.7±5.5	14.3± 1.9	< 0.005*
Visual Acuity (LogMar)			
Right eyes	4.2±1.4	0.92±0.2	< 0.005*
Left eyes	4.4±1.1	0.89±1.1	< 0.005*
Proportion of eyes with detectable SC-CSA			
Temporal quadrant n(%)	100/100 (200)	100/100 (200)	< 0.005*
Nasal quadrant n(%)	100/100 (200)	100/100 (200)	< 0.005*
Superior n(%)	100/100 (200)	100/100 (200)	< 0.005*
Inferior n(%)	100/100 (200)	100/100 (200)	< 0.005*
Percentage Eyes with measurement	100%	100%	

P < 0.05 is statistical significance.
POAG: primary open-angle glaucoma
Data presented as Mean±SD.
*Schlemm's canal was detectable in all the positions of the eye.
P < 0.05 is statistical significance

TABLE 6. The Parameter of S.C. in the POAG and normal control groups

Parameters	Normal Control (n= 50)	Patients POAG (n= 50)	*P*-Value*
Subject with observable (eyes)	100	100	
SC diameter/Length（μm）			
Average	42.736 ± 11.847	22.944 ± 97.548	<0.001*
Nasal quadrant	41.135± 10.510	21.855 ± 94.573	<0.001*
Temporal quadrant	38.432±12.186	21.281 ± 89.724	<0.001*
Superior	45.597±10.794	26.472 ± 10.436	<0.001*
Inferior	45.782±13.901	22.168 ± 10.154	<0.001*
S.C. wide （μm）			
Average	811.075 ± 352.022	499.801 ± 282.364	<0.001*
Nasal quadrant	785.200 ± 361.801	483.046 ± 361.801	<0.001*
Temporal quadrant	778.100 ± 329.081	469.669 ± 268.185	<0.001*
Superior	830.800 ± 323.268	514.901 ± 218.223	<0.001*
Inferior	850.200 ± 393.938	531.589 ± 281.250	<0.001*
S.C. area (μm^2)			
Average	26075 ± 12729	7069 ± 7370	<0.001*
Nasal quadrant	25210 ±11950	6172 ± 7798	<0.001*
Temporal quadrant	21940 ±11432	6139 ± 6733	<0.001*
Superior	28250 ± 12601	8901 ± 9161	<0.001*
Inferior	28900 ± 14933	7065 ± 5788	<0.001*
SC angle（°）			
Average	26.690 ± 7.717	29.114 ±10.522	0.09
Nasal quadrant	27.309 ± 9.051	29.392 ±11.165	0.106
Temporal quadrant	28.389 ± 9.217	29.710 ±10.890	0.271
Superior	24.849 ± 6.981	27.853 ±10.081	0.006
Inferior	26.216 ± 5.620	29.503 ± 9.952	<0.001*

POAG= Primary Open Angle Glaucoma SC = Schlemm's canal
*The Student t-test. There are significant statistical differences between normal people and POAG patients in Schlemm's canal angle in the superior and inferior ($p<0.05$)
*T- The test compared the schlemm's canal of 200 eyes from 100 normal subjects and 100 POAG eyes. It was found that there were significant statistical differences in the diameter, width, and area of the schlemm's canal between normal subjects and POAG patients ($p<0.05$)

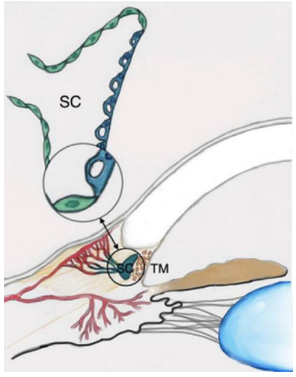

S.C. – Schlemm's Canal TM – Trabecular Meshwork

FIGURE 4. The Schlemm's canal: the outflow vessel (Lewczuk et al. 2022)

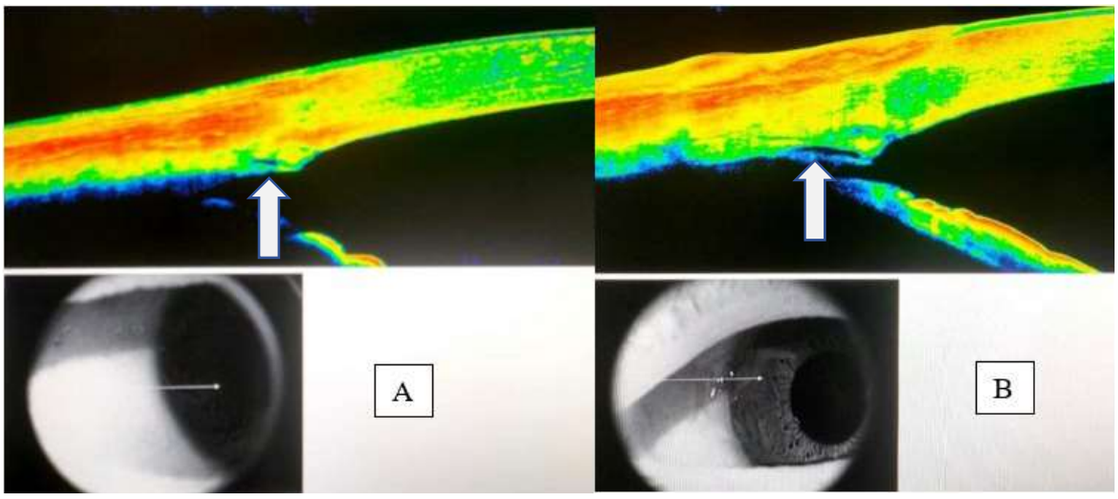

FIGURE 5. SD-OCT images of scanning side of S.C. in POAG eyes. The crypts and furrows of the iris are used to make a mark in the scanning guidelines to ensure the same scanning cross-section of S.C. before (a) and after (b) Modified suture Canaloplasty surgery. Morphology of S.C. before and after is marked by an arrow

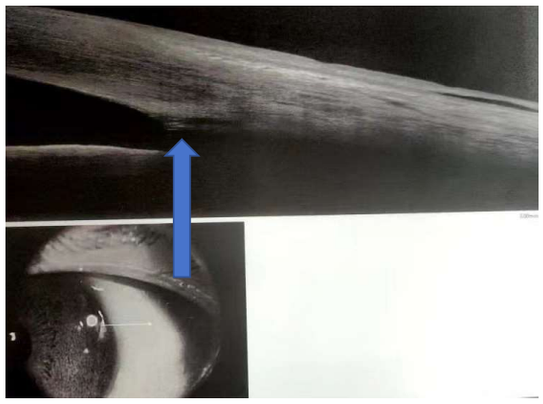

FIGURE 6. The arrow side (white colour) is suture canaloplasty, which can be imaged after canaloplasty surgery

CONCLUSIONS

The inner wall of the Schlemm canal would shear and herniate into the broth opening if intraocular pressure increased. Still, once intraocular pressure was normalized, the affected inner wall could exit through the collector aperture, allowing the Schlemm canal to function normally. The diameter of Schlemm's canal is shown in the study's results, along with all the essential factors contributing to the emergence of resistance in the canal. Nevertheless, neither visual acuity nor IOP seemed connected to any portion of Schlemm's canal jurisdiction. In line with previous European or elsewhere research, Schlemm's canal measurement in a Chinese population is consistent and does not deviate considerably from our findings. This research is valuable, and the measurement of Schlemm's canal area among the Asian population does not differ from other races.

Anterior Segment imaging OCT can be helpful in the Canaloplasty surgery procedure to find a correlation between preoperative and postoperative conditions and the Schlemm's canal area region. This would be a new development in Minimally Invasive Glaucoma Surgery and a new type of glaucoma surgery procedure to prevent blindness. Schlemm's canal has been extensively studied; our results also show that patients with POAG have a smaller SC area than normal people. These findings support the clinical utility of Schlemm's Canal region for assessing physiologic alterations in POAG patients and surgical planning, the surgical outcome of canaloplasty (Figures 5 & 6), and Minimally Invasive Glaucoma Surgery (MIGS) with involvement in Schlemm’s canal surgery.

ACKNOWLEDGMENTS

The authors thank Dr. Song Zhang from Biomedical Engineering in China for providing the Anterior Segment Optical Coherence Tomography imaging software tool. The authors declare that the research was conducted without any commercial or financial relationships that could be construed as a potential conflict of interest. This research was funded by the National Natural Science Foundation of China (Grant Number: 82101122), the Natural Science Foundation of Jiangsu Province (Grant Number: BK20201085), and the Clinical Capacity Improvement Project (Grant Number: JSPH-MB-2021-3). The funding organization had no role in the design or conduct of this research. ZLY and S contributed to the study concept, design, and manuscript. S and YL performed material preparation and data collection. LWG, SH, and SZL analyzed and interpreted the data. All authors read and approved the final manuscript.

FUNDING INFORMATION

This research was funded by the National Natural Science Foundation of China (Grant Number82101122) and the Clinical Capacity Improvemnet Project of Jiangsu Province Hospital (Grant Number JSPH-MB-2021-3).

CONFLICTS OF INTEREST

The authors declare no competing interests.

REFERENCES

Ainsworth, J.R. & Lee, W.R. 1990. Effects of age and rapid high-pressure fixation on the morphology of Schlemm's canal. *Investigative Ophthalmology & Visual Science* 31(4): 745-750.

Battista, S.A., Lu, Z., Hofmann, S., Freddo, T., Overby, D.R. & Gong, H. 2008. Reduction of the available area for aqueous humor outflow and increase in meshwork herniations into collector channels following acute IOP elevation in bovine eyes. *Investigative Ophthalmology & Visual Science* 49(12): 5346-5352.

Becker, B. 1958. The decline in aqueous secretion and outflow facility with age. *American Journal of Ophthalmology* 46(5 Part 1): 731-736.

Bentley, M.D., Hann, C.R. & Fautsch, M.P. 2016. Anatomical variation of human collector channel orifices. *Investigative Ophthalmology & Visual Science* 57(3): 1153-1159.

Boldea, R.C., Roy, S. & Mermoud, A. 2001. Ageing of Schlemm's canal in nonglaucomatous subjects. *International Ophthalmology* 24(2): 67-77.

Bourne, R.R., Stevens, G.A., White, R.A., Smith, J.L., Flaxman, S.R., Price, H., Jonas, J.B., Keeffe, J., Leasher, J., Naidoo, K., Pesudovs, K., Resnikoff, S., Taylor, H.R. & Vision Loss Expert Group. 2013. Causes of vision loss worldwide, 1990-2010: A systematic analysis. *The Lancet Global Health* 1(6): e339-e349.

Byszewska, A., Konopińska, J., Kicińska, A.K., Mariak, Z. & Rękas, M. 2019. Canaloplasty in the treatment of primary open-angle glaucoma: Patient selection and perspectives. *Clinical Ophthalmology* 13: 2617-2629.

Caprioli, J. 2007. Intraocular pressure fluctuation: An independent risk factor for glaucoma? *Archives of Ophthalmology* 125(8): 1124-1125.

Caprioli, J. & Coleman, A.L. 2008. Intraocular pressure fluctuation a risk factor for visual field progression at low intraocular pressures in the advanced glaucoma intervention study. *Ophthalmology* 115(7): 1123-1129.e3.

Chen, J., Huang, H., Zhang, S., Chen, X. & Sun, X. 2013. Expansion of Schlemm's canal by travoprost in healthy subjects determined by Fourier-domain optical coherence tomography. *Investigative Ophthalmology & Visual Science* 54(2): 1127-1134.

Chen, Y.P. 2014. A review of optical coherence tomography. *Journal of Value Engineering* 33(32): 255-256.

Day, A.C., Garway-Heath, D.F., Broadway, D.C., Jiang, Y., Hayat, S., Dalzell, N., Khaw, K.T. & Foster, P.J. 2013. Spectral domain optical coherence tomography imaging of the aqueous outflow structures in normal participants of the EPIC-Norfolk Eye Study. *The British Journal of Ophthalmology* 97(2): 189-195.

Dautriche, C.N., Tian, Y., Xie, Y. & Sharfstein, S.T. 2015. A closer look at Schlemm's canal cell physiology: Implications for biomimetics. *J. Funct. Biomater.* 6(3): 963-985.

Dvorak-Theobald, G. 1955. Further studies on the canal of Schlemm; its anastomoses and anatomic relations. *American Journal of Ophthalmology* 39(4 Pt 2): 65-89.

Fan, Y., Wei, J., Guo, L., Zhao, S., Xu, C., Sun, H. & Guo, T. 2020. Osthole reduces mouse IOP associated with ameliorating extracellular matrix expression of trabecular meshwork cell. *Investigative Ophthalmology & Visual Science* 61(10): 38.

Foster, P.J. & Johnson, G.J. 2001. Glaucoma in China: How big is the problem? *The British Journal of Ophthalmology* 85(11): 1277-1282.

Gao, K., Song, S., Johnstone, M.A., Zhang, Q., Xu, J., Zhang, X., Wang, R.K. & Wen, J.C. 2020. Reduced pulsatile trabecular meshwork motion in eyes with primary open angle glaucoma using phase-sensitive optical coherence tomography. *Investigative Ophthalmology & Visual Science* 61(14): 21.

Gong, H., Qi, H., Sun, W., Zhang, Y., Jiang, D., Xiao, J., Yang, X., Wang, Y. & Li, S. 2012. Design and synthesis of a series of pyrido[2,3-d]pyrimidine derivatives as CCR4 antagonists. *Molecules* 17(8): 9961-9970.

Grierson, I., Howes, R.C. & Wang, Q. 1984. Age-related changes in the canal of Schlemm. *Experimental Eye Research* 39(4): 505-512.

Hamanaka, T., Matsuda, A., Sakurai, T. & Kumasaka, T. 2016. Morphological abnormalities of Schlemm's canal in primary open-angle glaucoma from the aspect of aging. *Investigative Ophthalmology & Visual Science* 57(2): 692-706.

Hann, C.R., Bentley, M.D., Vercnocke, A., Ritman, E.L. & Fautsch, M.P. 2011. Imaging the aqueous humor outflow pathway in human eyes by three-dimensional micro-computed tomography (3D micro-CT). *Experimental Eye Research* 92(2): 104-111.

Hariri, S., Johnstone, M., Jiang, Y., Padilla, S., Zhou, Z., Reif, R. & Wang, R.K. 2014. Platform to investigate aqueous outflow system structure and pressure-dependent motion using high-resolution spectral domain optical coherence tomography. *Journal of Biomedical Optics* 19(10): 106013.

Hong, J., Xu, J., Wei, A., Wen, W., Chen, J., Yu, X. & Sun, X. 2013. Spectral-domain optical coherence tomographic assessment of Schlemm's canal in Chinese subjects with primary open-angle glaucoma. *Ophthalmology* 120(4): 709-715.

Johnstone, M. 2016. Intraocular pressure control through linked trabecular meshwork and collector channel motion. In *Glaucoma Research and Clinical Advances 2016 to 2018*, edited by Knepper, P.A. & Samples, J.R. Amsterdam: Kugler Publications.

Johnstone, M., Xin, C., Tan, J., Martin, E., Wen, J. & Wang, R.K. 2021. Aqueous outflow regulation - 21st century concepts. *Progress in Retinal and Eye Research* 83: 100917.

Kagemann, L., Wang, B., Wollstein, G., Ishikawa, H., Mentley, B., Sigal, I., Bilonick, R.A. & Schuman, J.S. 2015. Trabecular meshwork response to pressure elevation in the living human eye. *Journal of Visualized Experiments* 100: e52611.

Kagemann, L., Nevins, J. E., Jan, N. J., Wollstein, G., Ishikawa, H., Kagemann, J., Sigal, I.A., Nadler, Z., Ling, Y. & Schuman, J.S. 2014a. Characterisation of Schlemm's canal cross-sectional area. *Br. J. Ophthalmol.* 98(Suppl 2): ii10-ii14. doi:10.1136/bjophthalmol-2013-304629

Kagemann, L., Wang, B., Wollstein, G., Ishikawa, H., Nevins, J.E., Nadler, Z., Sigal, I.A., Bilonick, R.A. & Schuman, J.S. 2014b. IOP elevation reduces Schlemm's canal cross-sectional area. *Investigative Ophthalmol. Vis. Sci.* 55(3): 1805-1809. doi:10.1167/iovs.13-13264

Kagemann, L., Wollstein, G., Ishikawa, H., Sigal, I.A., Folio, L.S., Xu, J., Gong, H. & Schuman, J.S. 2011. 3D visualization of aqueous humor outflow structures *in-situ* in humans. *Experimental Eye Research* 93: 308-315.

Karl, M.O., Fleischhauer, J.C., Stamer, W.D., Peterson-Yantorno, K., Mitchell, C.H., Stone, R.A. & Civan, M.M. 2005. Differential P1-purinergic modulation of human Schlemm's canal inner-wall cells. *American Journal of Physiology Cell Physiology* 288(4): C784-C794.

Khatib, T.Z., Meyer, P.A.R., Lusthaus, J., Manyakin, I., Mushtaq, Y. & Martin, K.R. 2019. Hemoglobin video imaging provides novel *in vivo* high-resolution imaging and quantification of human aqueous outflow in patients with glaucoma. *Ophthalmology Glaucoma* 2(5): 327-335.

Kuehn, M.H., Vranka, J.A., Wadkins, D., Jackson, T., Cheng, L. & Ledolter, J. 2021. Circumferential trabecular meshwork cell density in the human eye. *Journal Exp. Eye Res.* 205: 108494.

Lai, J., Su, Y., Swain, D.L., Huang, D., Getchevski, D. & Gong, H. 2019. The role of Schlemm's canal endothelium cellular connectivity in giant vacuole formation: A 3D electron microscopy study. *Investigative Ophthalmology & Visual Science* 60(5): 1630-1643.

Lewczuk, K., Jabłońska, J., Konopińska, J., Mariak, Z. & Rękas, M. 2022. Schlemm's canal: The outflow 'vessel'. *Acta Ophthalmol.* 100(4): e881-e890. doi: 10.1111/aos.15027

Luo, X.G. 2010. *Human Anatomy (Systemic Anatomy).* 3rd ed. Beijing: Higher Education Press. p. 194.

Lusthaus, J.A., Khatib, T.Z., Meyer, P.A.R., McCluskey, P. & Martin, K.R. 2021. Aqueous outflow imaging techniques and what they tell us about intraocular pressure regulation. *Eye (London, England)* 35(1): 216-235.

Mansouri, K. & Shaarawy, T. 2015. Update on Schlemm's canal based procedures. *Middle East African Journal of Ophthalmology* 22(1): 38-44.

Osmond, M.J., Krebs, M.D. & Pantcheva, M.B. 2020. Human trabecular meshwork cell behavior is influenced by collagen scaffold pore architecture and glycosaminoglycan composition. *Biotechnology and Bioengineering* 117(10): 3150-3159.

Parc, C. & Johnson, D.H. 2003. Physiology of aqueous humor outflow resistance: Its relation to giant vacuoles. *J. Fr. Ophtalmol.* 26(2): 198-201 (Article in French).

Quigley, H.A. & Broman, A.T. 2006. The number of people with glaucoma worldwide in 2010 and 2020. *The British Journal of Ophthalmology* 90(3): 262-267.

Resnikoff, S., Pascolini, D., Etya'ale, D., Kocur, I., Pararajasegaram, R., Pokharel, G.P. & Mariotti, S.P. 2004. Global data on visual impairment in the year 2002. *Bulletin of the World Health Organization* 82(11): 844-851.

Shi, G., Wang, F., Li, X., Lu, J., Ding, Z., Sun, X., Jiang, C. & Zhang, Y. 2012. Morphometric measurement of Schlemm's canal in normal human eye using anterior segment swept source optical coherence tomography. *Journal of Biomedical Optics* 17(1): 016016.

Tamm, E.R., Braunger, B.M. & Fuchshofer, R. 2015. Intraocular pressure and the mechanisms involved in resistance of the aqueous humor flow in the trabecular meshwork outflow pathways. *Prog. Mol. Biol. Transl. Sci.* 134: 301-314.

Tham, Y.C., Li, X., Wong, T.Y., Quigley, H.A., Aung, T. & Cheng, C.Y. 2014. Global prevalence of glaucoma and projections of glaucoma burden through 2040: A systematic review and meta-analysis. *Ophthalmology* 121(11): 2081-2090.

UNP. 2022. *World Population Prospects*. https://population.un.org/wpp/ Accessed on 12 August 2023.

Vahabikashi, A., Gelman, A., Dong, B., Gong, L., Cha, E.D.K., Schimmel, M., Tamm, E.R., Perkumas, K., Daniel Stamer, W., Sun, C., Zhang, H.F., Gong, H. & Johnson, M. 2019. Increased stiffness and flow resistance of the inner wall of Schlemm's canal in glaucomatous human eyes. *Proceedings of the National Academy of Sciences of the United States of America* 116(52): 26555-26563.

Vranka, J.A., Kelley, M.J., Acott, T.S. & Keller, K.E. 2015. Extracellular matrix in the trabecular meshwork: Intraocular pressure regulation and dysregulation in glaucoma. *Experimental Eye Research* 133: 112-125.

Wang, F., Shi, G., Li, X., Lu, J., Ding, Z., Sun, X., Jiang, C. & Zhang, Y. 2012. Comparison of Schlemm's canal's biological parameters in primary open-angle Glaucoma and normal human eyes with swept source optical. *Journal of Biomedical Optics* 17(11): 116008.

Wong, T.Y., Loon, S.C. & Saw, S.M. 2006. The epidemiology of age related eye diseases in Asia. *The British Journal of Ophthalmology* 90(4): 506-511.

Xin, C., Wang, R.K., Song, S., Shen, T., Wen, J., Martin, E., Jiang, Y., Padilla, S. & Johnstone, M. 2017. Aqueous outflow regulation: Optical coherence tomography implicates pressure-dependent tissue motion. *Experimental Eye Research* 158: 171-186.

Xin, C., Johnstone, M., Wang, N. & Wang, R.K. 2016. OCT study of mechanical properties associated with trabecular meshwork and collector channel motion in human eyes. *PLoS ONE* 11(9): e0162048.

Yan, X., Li, M., Chen, Z., Zhu, Y., Song, Y. & Zhang, H. 2016a. Schlemm's canal and trabecular meshwork in eyes with primary open angle glaucoma: A comparative study using high-frequency ultrasound biomicroscopy. *PLoS ONE* 11(1): e0145824.

Yan, X., Li, M., Song, Y., Guo, J., Zhao, Y., Chen, W. & Zhang, H. 2016b. Influence of exercise on intraocular pressure, Schlemm's canal, and the trabecular meshwork. *Investigative Ophthalmology & Visual Science* 57(11): 4733-4739.

Zhu, J.Y., Ye, W., Wang, T. & Gong, H.Y. 2013. Reversible changes in aqueous outflow facility, hydrodynamics, and morphology following acute intraocular pressure variation in bovine eyes. *Chin. Med. J. (Engl)* 126(8): 1451-1457.

*Corresponding author; email: zhilanyuan@vip.sina.com